ISSN 1070-3284, Russian Journal of Coordination Chemistry, 2019, Vol. 45, No. 5, pp. 347–355. © Pleiades Publishing, Ltd., 2019.
Russian Text © The Author(s), 2019, published in Koordinatsionnaya Khimiya, 2019, Vol. 45, No. 5, pp. 297–305.

Magnetically Active 3*d* Metal Complexes with 3-Amino-4-Ethoxycarbonylpyrazole

L. G. Lavrenova[a, b, *], A. D. Ivanova[a, b], A. S. Bogomyakov[b, c], V. Yu. Komarov[a, b], and L. A. Sheludyakova[a, b]

[a] *Nikolaev Institute of Inorganic Chemistry, Siberian Branch, Russian Academy of Sciences, Novosibirsk, 630090 Russia*

[b] *Novosibirsk State University, Novosibirsk, 630090 Russia*

[c] *International Tomography Center, Siberian Branch, Russian Academy of Sciences, Novosibirsk, Russia*

**e-mail: ludm@niic.nsc.ru*

Received August 3, 2018; revised November 16, 2018; accepted November 19, 2018

Abstract—Coordination compounds of iron(II) and nickel(II) with 3-amino-4-ethoxycarbonylpyrazole (L), FeL_2A_2 (A = Cl^- (**I**), $C_2N_3^-$ (**II**)), $[FeL_2(NCS)_2(H_2O)_2]$ (**III**), and NiL_2Br_2 (**IV**), are synthesized. The compounds are studied by X-ray diffraction analysis, IR spectroscopy, and UV spectroscopy (diffuse reflectance spectra). A single crystal is observed for complex **III**, and its crystal structure is determined by X-ray structure analysis (CIF file CCDC no. 1857220). It is shown that L coordinates to the metal via the monodentate mode by the N(2) atom of the pyrazole cycle. The study of the temperature dependence $\mu_{eff}(T)$ in a temperature range of 2–300 K shows exchange interactions of the antiferro- or ferromagnetic character between the M^{2+} ions in the complexes. The type of exchange interactions depends on the composition of the compound.

Keywords: complexes, 3*d* metals, 3-amino-4-ethoxycarbonylpyrazole, IR spectra, X-ray diffraction analysis, X-ray structure analysis, diffuse reflectance spectra, magnetochemical study

DOI: 10.1134/S1070328419040055

INTRODUCTION

Coordination compounds capable of giving a response to a change in the external conditions attract attention of researchers. This class includes metal complexes with nitrogen-containing heterocyclic ligands. The spin crossover $^1A_1 \rightarrow {}^5T_2$ is observed in the 3*d* metal complexes with the d^4–d^7 electronic configuration of the octahedral or pseudo-octahedral structure of the coordination polyhedron. In these compounds the spin multiplicity changes at a certain ligand field strength under the action of the temperature, pressure, or light of a certain wavelength [1–3]. Exchange interactions of the antiferromagnetic and ferromagnetic character are observed between unpaired electrons of the metal ions in the Co(II), Ni(II), and Cu(II) complexes with nitrogen-containing ligands of the oligo- or polynuclear structure.

Cooperative interactions observed in the solid phase of the complexes are among the necessary conditions for magnetic phase transitions to occur. To obtain compounds with such properties, the paramagnetic centers should be connected by bridges: a chain of atoms or one bridging atom (ion). These chains (exchange channels) should not be extended in order to the distance between the metal ions would not be too long [4–6]. The search for new molecular ferromagnets is an important task of the modern chemistry. In A.L. Buchachenko's opinion, "ferromagnets belong to materials that constitute the foundation of modern civilization" [7]. A trend of the synthesis and study of the magnetically active metal complexes with paramagnetic ligands is developed in the works by R.Z. Sagdeev and V.I. Ovcharenko [6]. We searched for new magnetically active transition metal complexes containing diamagnetic polynitrogen-containing ligands.

Polynitrogen-containing heterocycles form a promising class of ligands for the synthesis of magnetically active compounds. In particular, the representative series of the 3*d* metal complexes with 1,2,4-triazoles were synthesized and studied. 1,2,4-Triazole and its derivatives, which have no substituents in the side chain capable of coordinating, attach to the metal predominantly via the bidentate-bridging mode due to which oligo- and/or polynuclear compounds are formed [3, 8, 9]. Spin crossover is observed in the iron(II) complexes with the ligands of this group [1, 3, 8], and the cobalt(II), nickel(II), and copper(II) polynuclear complexes manifest exchange interactions [6, 9]. These interactions are most often antiferromagnetic. At the same time, exchange interactions of the ferromagnetic character were found in a series of com-

pounds, in particular, in the Cu(II) and Ni(II) complexes with unsubstituted 1,2,4-triazole and 4-ethyl-, 4-amino-3,5-diphenyl-, and 4-(3,4-dichlorophenyl-1,2,4-triazoles [10–13].

Pyrazoles without substituents capable of coordinating attach to the metal predominantly via the monodentate mode by the N(2) atom of the heterocycle (unlike pyrazolate ions coordinating via to the bidentate-bridging mode similarly to 1,2,4-triazoles). Thus, atoms or groups of atoms potentially capable of exhibiting the bridging function are necessary for the preparation of oligo- and polynuclear compounds. The synthesis and study of the di- and tetranuclear copper(II) complexes with the pyrazole derivatives with antiferromagnetic exchange interactions were reported [14]. We have previously synthesized and studied the chloride compounds with 3-amino-4-ethoxycarbonylpyrazole (L) of the compositions ML_2Cl_2 (M = Co(II), Ni(II), Cu(II)) and CuL_2Br_2 [15, 16]. The complexes have the polynuclear chain structure due to the bridging function of the chloride and bromide ions. The study of the $\mu_{eff}(T)$ dependence in a temperature range of 2–300 K showed the ferromagnetic exchange interactions in the ML_2Cl_2 chloride complexes between the M^{2+} paramagnetic ions, whereas the transition to the magnetically ordered state with the Curie temperature $T_c \sim 10–12$ K was observed for CoL_2Cl_2 and NiL_2Cl_2. The replacement of the chloride ion by bromide in the CuL_2Hal_2 composition changes the character of the exchange interactions from ferromagnetic in CuL_2Cl_2 to antiferromagnetic in CuL_2Br_2.

It seemed reasonable to continue investigations in this direction. For this purpose, we synthesized and studied the magnetic properties of new Fe(II) and Ni(II) complexes with 3-amino-4-ethoxycarbonylpyrazole.

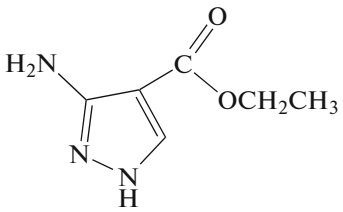

EXPERIMENTAL

The following reagents were used for the synthesis of the complexes: $NiBr_2 \cdot 3H_2O$ and KNCS (reagent grade), $FeCl_2 \cdot 4H_2O$ and $FeSO_4 \cdot 7H_2O$ (Acros Organics), 3-amino-4-ethoxycarbonylpyrazole (L) and NaC_2N_3 (Aldrich), and ethanol (rectificate).

Synthesis of FeL_2Cl_2 (I). Ascorbic acid (0.2 g) and $FeCl_2 \cdot 4H_2O$ (0.001 mol, 0.20 g) were dissolved together in a mixture of ethanol (5 mL) and water (2 mL), and the solution was acidified with concentrated HCl (2 droplets). Ligand L (0.002 mol, 0.31 g) was dissolved in ethanol (5 mL), and the solution of the ligand was added to the solution of $FeCl_2$. The resulting solution was evaporated in a water bath to the precipitation onset and cooled in a crystallizer with ice. The white precipitate formed was filtered off on the Schott filter (16 pores), washed two times with small portions of ethanol, and dried in air. Other precipitates were filtered off and dried similarly. The yield was 0.36 g (82%).

For $C_{12}H_{18}N_6O_4Cl_2Fe$ (**I**)			
Anal. calcd., %	C, 33.0	H, 4.2	N, 19.2
Found, %	C, 33.1	H, 4.3	N, 19.4

Synthesis of $FeL_2(C_2N_3)_2$ (II). Ascorbic acid (0.2 g) and $FeSO_4 \cdot 7H_2O$ (0.001 mol, 0.28 g) were dissolved together in water (8 mL) on heating, NaC_2N_3 (0.006 mol, 0.53 g) was added to the solution, and the resulting mixture was stirred to the complete dissolution of NaC_2N_3. Then a solution of L (0.002 mol, 0.32 g) in ethanol (6 mL) was poured. The solution was evaporated to 1/2 of the initial volume in a water bath and cooled in a crystallizer with ice. The white precipitate formed was filtered off and washed with water and ethanol. The yield was 0.44 g (88%).

For $C_{16}H_{18}N_{12}O_4Fe$ (**II**)			
Anal. calcd., %	C, 38.6	H, 3.6	N, 33.7
Found, %	C, 38.4	H, 3.5	N, 33.6

Synthesis of $[FeL_2(NCS)_2(H_2O)_2]$ (III). Ascorbic acid (0.2 g) and $FeSO_4 \cdot 7H_2O$ (0.0005 mol, 0.14 g) were dissolved together in water (5 mL) on heating, KNCS (0.003 mol, 0.29 g) was added to this solution, which was stirred to the complete dissolution of KNCS, and a solution of L (0.003 mol, 0.47 g) in ethanol (6 mL) was poured. The solution was evaporated to 1/2 of the initial volume and cooled in a crystallizer with ice. The white precipitate formed was filtered off and washed with water and ethanol. The yield was 0.27 g (52%). Single crystals of the complex were obtained from the mother liquor by the slow evaporation of the solvent.

For $C_{14}H_{22}N_8O_6S_2Fe$ (**III**)			
Anal. calcd., %	C, 32.4	H, 4.3	N, 21.6
Found, %	C, 32.7	H, 4.2	N, 21.5

Synthesis of NiL_2Br_2 (IV). Nickel salt $NiBr_2 \cdot 3H_2O$ (0.003 mol, 0.82 g) was dissolved in ethanol (7 mL), and L (0.003 mol, 0.47 g) was dissolved in ethanol (5 mL) on heating. The solutions were mixed, and a solvent excess was removed by evaporation to 1/3 of the initial volume in a water bath. The yellow-green

Table 1. Positions of the observed reflections in the diffraction patterns of the polycrystalline samples of compounds **I**–**IV** in the 2θ range 5°–20° (CuK_α)*

Sample	2θ, deg
I	<**5.00**; 9.56; **14.12**; **14.36**; 16.32; 16.61; 19.85
II	12.59; 13.08; 13.48; **14.53**; 15.80; 16.56; 17.14; 18.52
III	**12.34**; 14.12; 15.09; 16.42; 17.55; 18.88; 19.76
IV	**5.08**; **9.64**; 10.20; 13.04; 13.20; **13.70**; **14.48**; 15.36; **16.58**; 19.10; **19.97**

* Intense reflections are given in bold.

precipitate formed was filtered off and washed with water and ethanol. The yield was 0.24 g (43%).

For $C_{12}H_{18}N_6O_4Br_2Ni$ (**IV**)			
Anal. calcd., %	C, 27.3	H, 3.4	N, 15.9
Found, %	C, 26.9	H, 3.6	N, 15.4

Elemental analyses of the complexes were carried out on a EURO EA 3000 instrument (EuroVector, Italy) at the Analytical Laboratory of the Nikolaev Institute of Inorganic Chemistry (Siberian Branch of the Russian Academy of Sciences).

The X-ray diffraction analysis of polycrystalline samples was conducted on a Shimadzu XRD 7000 diffractometer (CuK_α radiation, Ni filter, scintillation detector) at room temperature. The samples were triturated in heptane and deposited on the polished side of the quartz cell. Detection was carried out in an angular range of 5°–60° with an increment of 0.03° and an exposure of 1 s/point. Narrow diffraction peaks indicating the crystalline phases were observed on all diffraction patterns. The positions of the observed reflections in the 2θ range from 5° to 20° are presented in Table 1. The experimental diffraction patterns and a number of diffraction patterns calculated from the known structural models are compared in the Topas Academic version 6 program [17]. All diffraction patterns have no diffraction reflections from the structurally characterized starting reactants (CIF files CCDC nos. 631805 (L) and 143569 (NaC_2N_3); ICSD nos. 16589 ($FeSO_4 \cdot 7H_2O$) and 9198 ($FeCl_2 \cdot 4H_2O$)) and possible inorganic reaction products of the ion exchange and a change in the hydrate number (ICSD nos. 15597 ($FeCl_2 \cdot 2H_2O$), 249781 ($Na_2SO_4 \cdot 7H_2O$), 249782 ($Na_2SO_4 \cdot 8H_2O$), and 30505 ($Na_2SO_4 \cdot 10H_2O$). The diffraction pattern of compound **III** is consistent with that calculated for the structure of $FeL_2(NCS)_2(H_2O)_2$ described in this article with the unit cell parameters a = 22.459(7), b = 7.041(2), c = 14.912(4) Å, β = 105.63(3)°, and V = 2271(1) Å^3.

The X-ray structure analysis of the crystal of compound **III** was conducted using a standard procedure on a Bruker APEX Duo automated four-circle diffractometer with a two-coordinate CCD detector (MoK_α, λ = 0.71073 Å, graphite monochromator). The main crystallographic data and refinement details are presented in Table 2. The data were processed using the APEX 2 program package [18]. An absorption correction was applied empirically from equivalent reflection intensities (SADABS). The structure was solved by a direct method and refined by full-matrix least squares for F^2 in the anisotropic approximation for all nonhydrogen atoms using the SHELXTL program package [18, 19] and the OLEX2 graphical shell [20]. The hydrogen atoms of 2-methyl-1,2,4-triazolo[1,5-*a*]benzimidazole were specified geometrically and refined by the riding model. The hydrogen atoms of the water molecules were localized from the difference Fourier synthesis and refined in the isotropic approximation with the fixed values $U_{iso}(H) = 1.5U_{eq}(O)$. The coordinates of atoms and thermal parameters were deposited with the Cambridge Crystallographic Data Centre (CIF file CCDC no. 1857220; http://www ccdc.cam.ac.uk/data_request/cif).

IR absorption spectra were recorded on Scimitar FTS 2000 and Vertex 80 spectrometers in a range of 4000–100 cm^{-1}. The samples were prepared as suspensions in Nujol, fluorinated oil, and polyethylene. Diffuse reflectance (DR) spectra were recorded on a UV-3101 PC scanning spectrometer (Shimadzu) at room temperature.

The magnetic properties of polycrystalline samples were studied on an MPMS-*XL* SQUID magnetometer (Quantum Design) in a temperature range of 2–300 K and a magnetic field of 5 kOe. Diamagnetic corrections were applied according to Pascal's additive scheme to calculate the paramagnetic component of the molar magnetic susceptibility (χ). The effective magnetic moment (μ_{eff}) in the paramagnetic region was determined by the equation

$$\mu_{eff} = \left(\frac{3k}{N_A\mu_B^2}\chi T\right)^{1/2} \approx (8\chi T)^{1/2},$$

where k is the Boltzmann constant, N_A is Avogadro number, and μ_B is Bohr magneton.

RESULTS AND DISCUSSION

Complexes **I**–**IV** were isolated from aqueous-ethanol solutions at different M : L ratios (depending on the metal and anion). The iron(II) compounds were

Table 2. Main crystallographic experimental data for the structure of compound **III**

Parameter	Value
FW	518.36
a, Å	22.411(10)
b, Å	7.0325(3)
c, Å	14.7646(8)
β, deg	104.611(2)
Space group	*C*2/*c*
Z	4
Crystal size, mm	0.32 × 0.16 × 0.10
V, Å^3	2251.7(2)
ρ_{calcd}, g/cm^3	1.529
μ, mm^{-1}	0.903
Number of measured/ independent reflections	7417/2907
Number of refined parameters	157
R_{int}/R_σ	0.0234/0.0309
GOOF	1.079
R_1/wR_2 for $I > 2\sigma(I)$	0.0362/0.0794
R_1/wR_2 for all data	0.0486/0.0856
Residual electron density (min/max), e Å^{-3}	−0.30/0.54

obtained in the presence of ascorbic acid as a reducing and a weakly acidifying agent.

According to the X-ray structure analysis data, the iron(II) ion in the molecular complex $[FeL_2(NCS)_2(H_2O)_2]$ (Fig. 1) is located in the inversion center. The coordination mode FeN_4O_2 with the geometry of a weakly distorted octahedron is formed by the nitrogen atoms of two pyrazole ligands (N(11) and N(1) of the pyrazole cycle according to the IUPAC numeration), the N(1) nitrogen atoms of the thiocyanate ions, and two O(1) oxygen atoms of the water molecules. According to the symmetry, all ligands of the same type exist in the *trans* positions. Selected bond lengths and bond angles in the structure of compound **III** and a comparison of them with the CCDC data [21] are presented in Table 3. The average values and standard deviations of the bond lengths are given to search for the Fe(II) complexes with the pyrazole-containing ligands (Fe–N(L)), the Fe(II) compounds with NCS and the coordinated nitrogen atom (Fe–N(NCS)), and the Fe(II) complexes with the aqua ligands (Fe–O). The Fe–O distance in complex **III** is typical of the Fe(II) complexes with the aqua ligands. The Fe–N(NCS) distance is a slightly longer than the distances known at the moment. The Fe–N(L) distance falls onto the second maximum of the bimodal distribution indicating the high-spin state of Fe(II) in complex **III**. The geometric characteristics of ligand L are close to those determined earlier for the complexes with other central atoms [22]. The elongation of the atomic shift ellipsoid for the nitrogen atom of the amino group indicates the absence of a complete conjugation with the aromatic system, which is characteristic of other studied structures with similar fragments [22] and is confirmed by the quantum chemical calculations [23]. The conformation of ligand L in complex **III** is stabilized by the intramolecular hydrogen bond between the amino group and carboxylic oxygen atom (Fig. 2a).

The structure of compound **III** contains chains formed by the hydrogen bonds between the carboxylic oxygen atom and hydrogen atoms of the amino group and pyrazole ring arranged along the crystallographic direction *b* (Fig. 2a). A strong intermolecular interaction can be assumed between the amino groups of one chain and carboxyl groups of another chain leading to the formation of layers parallel to the *ab* plane consisting of the hydrogen-bonded chains (Fig. 2b). The shortest distances between the non-hydrogen atoms of two adjacent molecules *A* and *B* from the same layer are C(14*A*)–N(13*B*) 3.459(4) and O(12*A*)–N(13*B*) 3.574(3) Å (Fig. 2c). A similar interaction between the molecules from different layers are less favorable, most likely, because of approaching two amino groups and two carboxyl groups: N(13*A*)–N(13*B*) 4.111(4), O(12*A*)–O(12*B*) 3.838(3), and O(12*A*)–C(14*B*) 3.793(3) Å (Fig. 2d).

The vibrational frequencies and their assignment for the functional groups of ligand L and complexes **I**–**IV** are presented in Table 4. The high-frequency range of the IR spectrum of L contains the narrow $\nu(NH_2)$ band at 3480 cm^{-1} and also a broad structured band in a range of 3300–2400 cm^{-1} indicating the presence of hydrogen bonds, whose formation can involve the NH, NH_2, and C=O groups. In the spectra of all complexes, the ν(NH) bands undergo a high-frequency shift compared to their positions in the spectrum of ligand L, most likely, due to a change in the character of the hydrogen bonds upon complex formation. The ν(C=O) bands also shift to the high-energy range indicating no coordination of the C=O groups to the metal ion. The character of the spectra in the range of ring vibrations and the appearance of the bands in the low-frequency range, which were absent from the spectrum of ligand L (Table 4), which can be assigned to ν(M–N), indicate the coordination of the nitrogen atoms of the pyrazole ring to the metal. In the IR spectrum of complex **II**, the $\nu(N(CN)_2^-)$ bands of the anions shift to both the low- and high-frequency ranges indicating that this anion enters into the composition of the coordination mode of the Fe^{2+} ion. The IR spectrum of complex **III** exhibits the splitting and noticeable shift of the $\nu(NCS^-)$ band to the range of high energies compared to the spectrum of salt KNCS [24]. This indicates the coordination of the thiocyanate ion to Fe^{2+}, which is consistent with the X-ray structure analysis data.

The bands at 173 and 145 cm^{-1} assigned to the ν(M–Cl) and ν(M–Br) vibrations, respectively, are observed in the low-frequency spectral ranges of complexes **I** and **IV**. The positions of these bands assume the bridging coordination mode of the halide ions to the metal ions and the formation of chain polynuclear compounds **I** and **IV**. This is indicated by a substantial shift of the ν(M–Cl) and ν(M–Br) bands in the IR spectra of compounds **I** and **IV** in a range of 600–100 cm^{-1} to the range of low energies compared to their positions in the spectra of the complexes containing coordinated terminal halide ions.

The DR spectra of iron(II) complexes **I**–**III** exhibit the bands that can be assigned to the *d*–*d* transition $^5T_2 \rightarrow {}^5E$ in a weak distorted octahedral ligand field (Table 5). The positions of maxima of these bands at 10638 (**I**), 11669 (**II**), and 11933 cm^{-1} (**III**) agree with the published data for the high-spin octahedral iron(II) complexes with the nitrogen-containing ligands [3, 25]. Our data obtained earlier for the M(II) complexes with L (including the X-ray structure analysis data [16]), the determination of the crystal structure of complex **III** in this work, and the present analysis of the IR spectra of complexes **I**–**IV** indicate the monodentate coordination mode of L in all compounds. The coordination modes in compounds **I**, **II**, and **IV** are supplemented to octahedral ones due to the bridging function of the Cl^-, $N(CN)_2^-$, and Br^- ions, respectively.

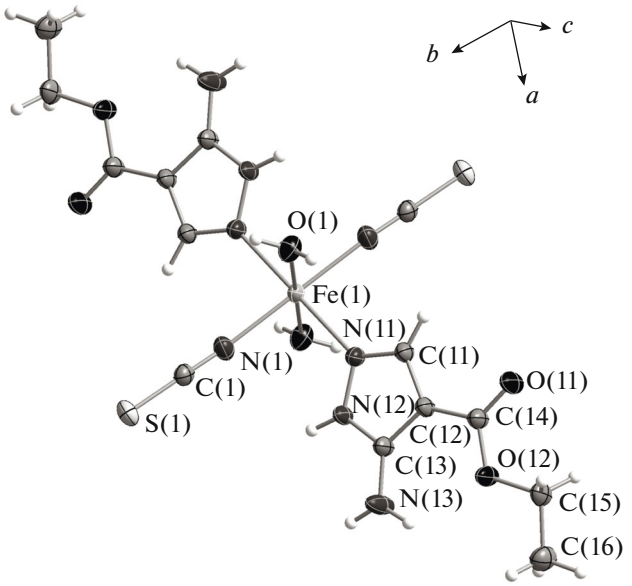

Fig. 1. Structure of the $[FeL_2(H_2O)_2(NCS)_2]$ complex. Atomic shift ellipsoids are presented for 50% probability.

An analysis of the spectra of $NaN(CN)_2$ and complex **II** and a comparison with the literature data for the complexes with the nitrogen-containing ligands and dicyanamide ions in which the anion is coordi-

Table 3. Selected bond lengths and bond angles in the structure of compound **III** compared with the published data [21]

Bond length/angle	*d*, Å/ω, deg	Distributions in CCDC (number of correspondences in braces)
Fe–N(L)	2.151(2)	1.98(3) and 2.18(4) {603}
Fe–N(NCS)	2.140(2)	1.90–2.12 {3}
Fe–O	2.142(2)	2.11(6) {267}
N(L)FeN(NCS)	90.33(6)/89.67(6)	
N(L)FeO	92.47(6)/87.53(6)	
N(NCS)FeO	92.20(7)/87.80(7)	

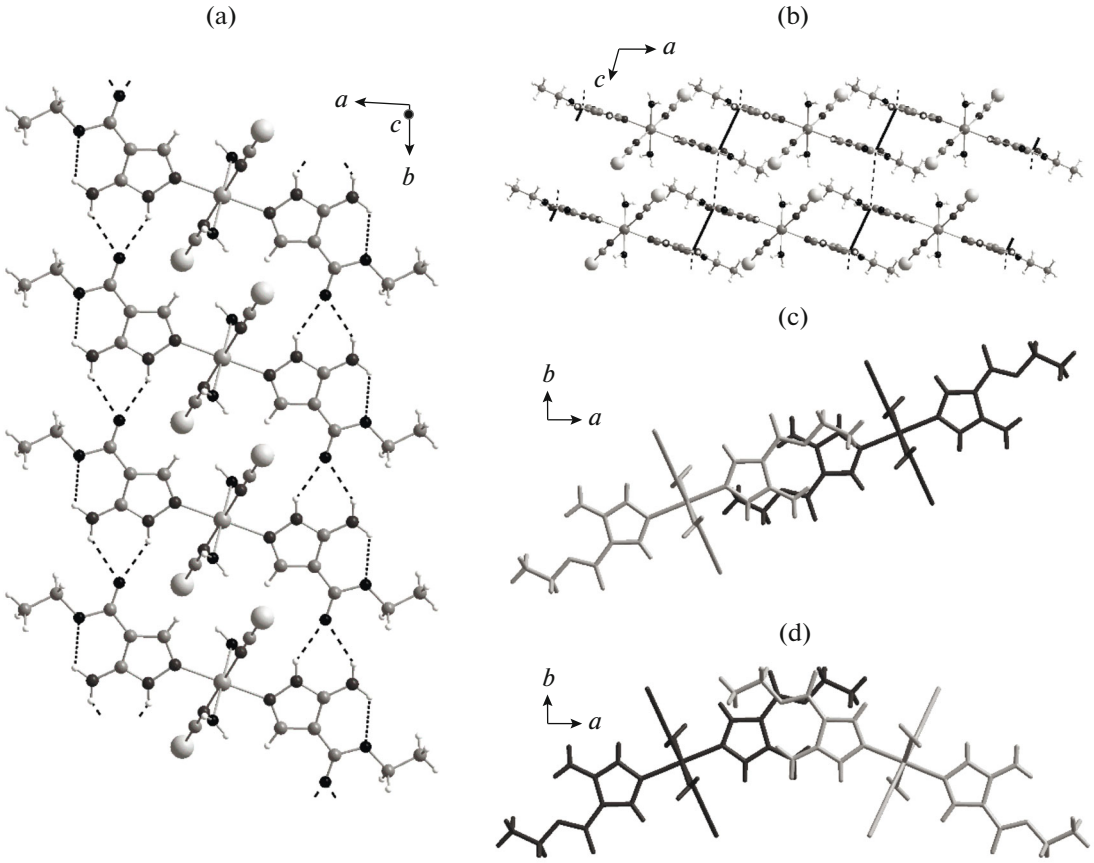

Fig. 2. (a) Hydrogen-bonded chains along the *b* axis and the differences in intermolecular contacts between the organic ligands from different chains: (b) the view along the hydrogen-bonded chains, (c) the $-NH_2...-COO-$ contacts between the chain from the same "layer," and (d) the $-NH_2...-NH_2$ and $-COO-...-COO-$ contacts between the chains from different layers.

nated to the metal via the bidentate-bridging mode [26–29] show that the character of band shifting upon anion coordination to the metal indicates the bidentate-bridging coordination mode of this anion.

The $\mu_{eff}(T)$ and $1/\chi(T)$ dependences for complex **I** are presented in Fig. 3. At 300 K $\mu_{eff} = 5.55\ \mu_B$. With decreasing temperature μ_{eff} gradually increases to 14.15 μ_B at 14 K after which decreases sharply to 9.73 μ_B at 5 K. The $1/\chi(T)$ dependence in a temperature range of 300–50 K is described by the Curie–Weiss law with the optimum values of the Curie (C) and Weiss (θ) constants equal to 3.51 K cm^3/mol and 29.7 K, respectively. The high-temperature value of μ_{eff} and the Curie constant are somewhat higher than the theoretical spin-only values equal to 4.90 μ_B and 3.00 cm^3/mol, respectively, for the Fe^{2+} ion. An increase in μ_{eff} with decreasing temperature and the positive Weiss constant indicate exchange interactions of the ferromagnetic character in compound **I**. A decrease in μ_{eff} at temperatures lower than 14 K can be related to the saturation effects in the magnetic field and/or weaker exchange interactions of the antiferromagnetic character.

The $\mu_{eff}(T)$ dependence for complex **III** is presented in Fig. 4. The value of μ_{eff} at 340 K is 5.19 μ_B and remains almost unchanged with decreasing temperature to 290 K, after which a slight decrease (to 5.10 μ_B) is observed at 230 K. On further cooling μ_{eff} remains unchanged down to 50 K and then decreases to 4.25 μ_B at 5 K. The high-temperature value of μ_{eff} agrees with the theoretical spin-only value equal to 4.97 μ_B for one Fe^{2+} ion with spin $S = 2$ at a g factor of 2.

The $\mu_{eff}(T)$ and $1/\chi(T)$ dependences for complex **IV** are presented in Fig. 5. At 300 K $\mu_{eff} = 2.90\ \mu_B$, and with decreasing temperature μ_{eff} gradually increases to 3.27 μ_B at 5 K. The $1/\chi(T)$ dependence in a range of 300–50 K is described by the Curie–Weiss law with the optimum values of the Curie (C) and Weiss (θ) constants equal to 1.02 K cm^3/mol and 8.4 K, respectively. The high-temperature value of μ_{eff} and the Curie constant are well consistent with theoretical spin-only values of 2.83 μ_B and 1.00 cm^3/mol, respectively, for the Ni^{2+} ion.

Table 4. Main vibrational frequencies in the spectra of L, complexes **I**–**IV**, $Na(N(CN)_2)$, and KNCS

ν, cm^{-1}							
L	**I**	**II**	**III**	**IV**	$NaN(CN)_2$	KNCS	Assignment
3480 3295 sh 3238 3203	3483 3461 3355 3335	3496 3376 3344 3280	3491 3371 br 3322 sh 3211	3457 3424 3353 3314			$\nu(NH_2)$ $\nu(NH)$ $\nu(OH) + \nu(NH)$ (for 3)
3049 2980 2905 2861	3088 2978 2925 2859	3080 2995 2959 2901	3074 2997 2964 2899	3079 2989 2934 2857			$\nu(CH)_{ring}$ $\nu(CH)_{OC_2H_5}$
		2292 2237 2175			2287 2233 2182		$\nu_s + \nu_{as}(C{-}N)$ $\nu_{as}(C{\equiv}N)$ $\nu_s(C{\equiv}N)$
			2106 2057			2053	$\nu(NCS^-)$
1672 1621	1694 1623	1686 1627	1667 1628	1685 1619			$\nu(C{=}O)$ $\delta(NH_2)$
1557 1521 1502	1571	1561 1545	1562 1548	1561			R_{ring}
	229	247	234, 255	246			$\nu(M{-}N)$
	173			145			$\nu(M{-}Hal)$

Table 5. DR spectral parameters for complexes **I**–**IV**

Compound	λ_{max}, nm	Band assignment
FeL_2Cl_2 (**I**)	940	$^5T_2 \rightarrow {}^5E$
$FeL_2(C_2N_3)_2$ (**II**)	857	$^5T_2 \rightarrow {}^5E$
$[FeL_2(H_2O)_2(NCS)_2]$ (**III**)	838	$^5T_2 \rightarrow {}^5E$
NiL_2Br_2 (**IV**)	722 1292	$^3A_2 \rightarrow {}^3T_1(F)$ $^3A_2 \rightarrow {}^3T_2$

An increase in $\mu_{eff}(T)$ with decreasing temperature and a positive value of the Weiss constant indicate the predomination of exchange interactions of the ferromagnetic character between spins of the Ni^{2+} ions.

Thus, we synthesized and characterized a series of new Fe(II) and Ni(II) complexes with 3-amino-4-ethoxycarbonylpyrazole. The exchange interactions of the antiferromagnetic character are observed in complex **III** between the Fe^{2+} ions, and the exchange interactions of the ferromagnetic character are observed in complexes **I** and **IV** between the Fe^{2+} and Ni^{2+} ions, respectively.

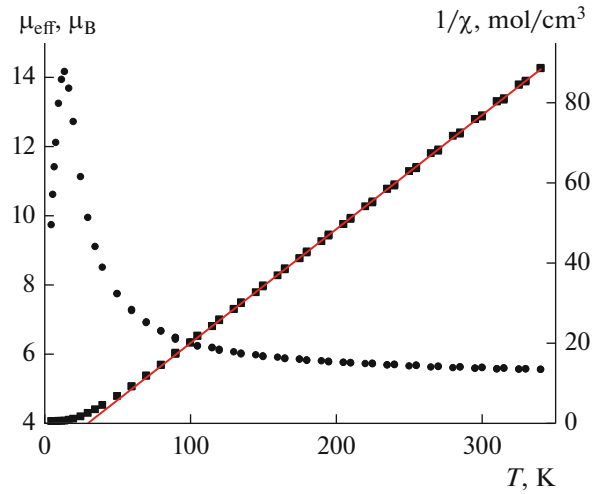

Fig. 3. Dependences (●) $\mu_{eff}(T)$ and (■) $1/\chi(T)$ for FeL_2Cl_2 (**I**).

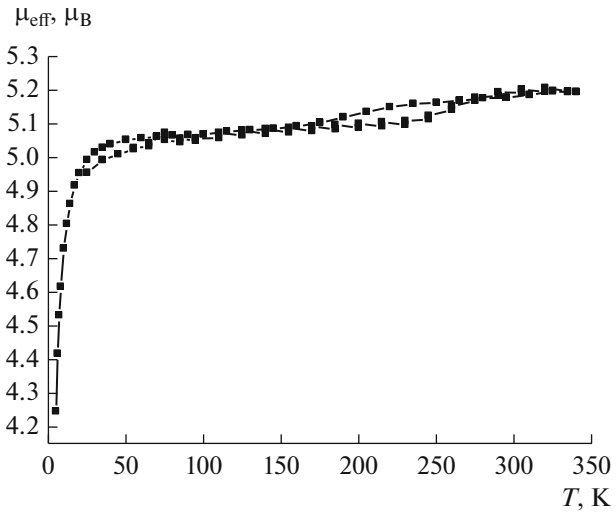

Fig. 4. Dependence $\mu_{eff}(T)$ for $[FeL_2(H_2O)_2(NCS)_2]$ (**III**).

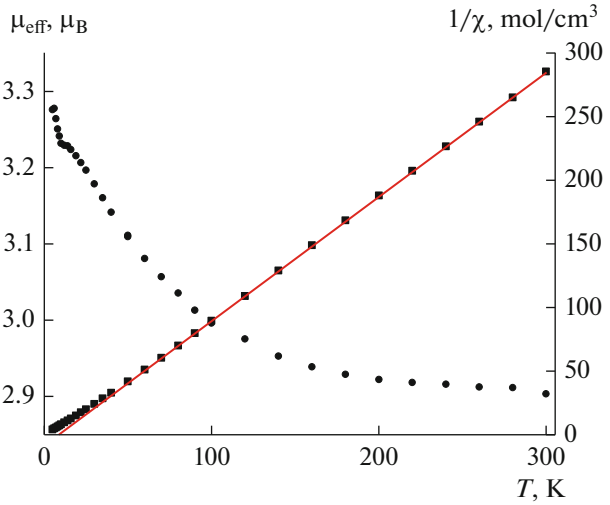

Fig. 5. Dependences (●) $\mu_{eff}(T)$ and (■) $1/\chi(T)$ for NiL_2Br_2 (**IV**).

ACKNOWLEDGMENTS

The authors are grateful to I.V. Yushina for DR spectra recording and to N.P. Korotkevich for obtaining diffraction patterns.

FUNDING

This work was supported by the Russian Foundation for Basic Research, projects nos. 16-53-00020 Bel_a and 18-53-00006 Bel_a.

REFERENCES

1. *Spin Crossover in Transition Metal Compounds I–III*, Gutlich, P. and Goodwin, H., Eds., Top Curr. Chem. Springer, 2004, vols. 233–235.
2. Halcrow, M.A., *Spin-Crossover Materials Properties and Applications*, UK: Wiley, 2013.
3. Lavrenova, L.G. and Shakirova, O.G., *Eur. J. Inorg. Chem.*, 2013, nos. 5–6, p. 670.
4. Inoue, M. and Kubo, M., *Coord. Chem. Rev.*, 1976, vol. 21, no. 1, p. 1.
5. Buchachenko, A.L., *Usp. Khim.*, 1990, vol. 59, no. 4, p. 529.
6. Ovcharenko, V.I. and Sagdeev, R.Z., *Usp. Khim.*, 1999, vol. 68, p. 381.
7. Buchachenko, A.L., *Izv. Akad. Nauk. Ser. Khim.*, 2011, no.12, p. 2393.
8. Lavrenova, L.G. and Larionov, S.V., *Koord. Khim.*, 1998, vol. 24, no. 6, p. 403.
9. Haasnoot, J.G., *Coord. Chem. Rev.*, 2000, vols. 200–202, p. 131.
10. Engelfried, D.W., Groeneveld, W.L., and Nap, G.M., *Z. Naturforsch., A: Phys. Sci.*, 1980, vol. 35, p. 1382.
11. Vos, G., Haasnoot, J.G., Verschoor, C.C., et al., *Inorg. Chim. Acta*, 1985, vol. 105, p. 31.
12. Bushuev, M.B., Virovets, A.V., Naumov, D.Yu., et al., *Russ. J. Coord. Chem.*, 2006, vol. 32, no. 5, p. 309. doi 10.1134/S1070328406050010
13. Lider, E.V., Lavrenova, L.G., Shvedenkov, Yu.G., et al., *Russ. J. Coord. Chem.*, 2007, vol. 33, no. 1, p. 37. doi 10.1134/S107032840701006X
14. Keij, F.S., Haasnoot, J.G., Oosterling, A.J., et al., *Inorg. Chim. Acta*, 1991, vol. 181, p. 185.
15. Lavrenova, L.G., Zhilin, A.S. Bogomyakov, A.S., et al., *J. Struct. Chem.*, 2013, vol. 54, no. 4, p. 713.
16. Lavrenova, L.G., Ivanova, A.D., Bogomyakov, A.S., et al., *Russ. J. Coord. Chem.*, 2015, vol. 41, no. 2, p. 86.
17. Coelho, A.A., *J. Appl. Crystallogr.*, 2018, vol. 51, p. 210.
18. APEX2 (version 1.08), SAINT (version 7.03), SADABS (version 2.11), SHELXTL (version 6.12), Madison: Bruker AXS Inc., 2004.
19. Sheldrick, G.M., *Acta Crystallogr., Sect. C: Struct. Chem.*, 2015, vol. 71, p. 3.
20. Dolomanov, O.V., Bourhis, L.J., Gildea, R.J., et al., *J. Appl. Crystallogr.*, 2009, vol. 42, p. 339.
21. Groom, C.R., Bruno, I.J., Lightfoot, M.P., and Ward, S.C., *Acta Crystallogr., Sect. B: Struct. Sci., Cryst. Eng. Mater.*, 2016, vol. 72, p. 171.

22. Berezin, A.S., Ivanova, A.D., Komarov, V.Yu., et al., *New J. Chem.*, 2018, vol. 42, p. 4902.

23. Sukhikh, T.S., Komarov, V.Yu., Konchenko, S.N., and Benassi, E., *Polyhedron*, 2018, vol. 139, p. 33.

24. Nakamoto, K., *Infrared Spectra and Raman Spectra of Inorganic and Coordination Compounds*, New York: Wiley, 1986.

25. Lever, A.B.P., *Inorganic Electronic Spectroscopy*, Amsterdam: Elsevier, 1987, vol. 2.

26. De La Pinta, N., Martin, S., and Urtiaga, M.K., *Inorg. Chem.*, 2010, vol. 49, no. 22, p. 10445.

27. Kohler Von, H., Kolbe, A., and Lux, G., *Z. Anorg. Allg. Chem.*, 1977, vol. 428, p. 103.

28. Mautner, F.A., Traber, M., Fischer, R.C., et al., *Polyhedron*, 2017, vol. 138, p. 13.

29. Vangdal, B., Carranza, J., Lloret, F., et al., *Dalton Trans.*, 2002, p. 566.

Translated by E. Yablonskaya